Int J Adv Manuf Technol (2009) 44:955–968
DOI 10.1007/s00170-008-1911-9

ORIGINAL ARTICLE

Numerical modeling of the influence of process parameters and workpiece hardness on white layer formation in AISI 52100 steel

D. Umbrello · I. S. Jawahir

Received: 30 September 2008 / Accepted: 18 December 2008 / Published online: 10 January 2009

Abstract White layer formation is considered to be one of the most important aspects to take into account in hard machining. Therefore, a large number of experimental investigations have been carried out in recent times on the formation mechanisms and properties of the white layer. However, up to now, only very few studies have been reported on modeling of the white layer formation. This paper presents a finite element model which predicts the white layer formation during machining of hardened AISI 52100 steel. This numerical model was properly calibrated by means of an iterative procedure based on the comparison between experimental and numerical data. The empirical model was also validated for a range of cutting speeds, uncut chip thickness, and material hardness values. This study provides excellent results concerning cutting force, temperature, chip morphology, and white layer. From this study, it was also possible to properly analyze the influence of process variables on the white layer formation.

Keywords Hard machining · White layer · Finite element analysis

D. Umbrello (✉)
Department of Mechanical Engineering, University of Calabria, Rende 87036 CS, Italy
e-mail: d.umbrello@unical.it
URL: www.unical.it

I. S. Jawahir
Department of Mechanical Engineering, University of Kentucky, Lexington, KY 40506, USA
e-mail: jawahir@engr.uky.edu
URL: www.mfg.uky.edu/mach_lab

1 Introduction

In recent times, significant interest has been generated within the research community with the new understanding of the microstructure changes observed in the surface layers of machined hardened steels—commonly referred to as white layer. This layer is typically a few microns thickness and is hard and brittle. Due to the general conviction that these microstructure changes are disadvantageous to fatigue life of the part, white layer is commonly removed from parts before usage.

Over the years, although a number of experimental investigations were carried out in order to understand the formation mechanisms and properties of white layer in machining and grinding, only very few studies can be found in literature on modeling of white layer formation in machining of hardened steels. Akcan [1, 2] and Chou and Evans [3] used an analytical approach to predict white layer formation by assuming that it is due to thermally driven phase transformation effects.

Therefore, in order for manufacturers to maximize their gains from utilizing hard finish turning, it is desirable to develop models that are capable of predicting the beginning of the white layer formation as a function of the machining conditions. The goal could be the identification of cutting conditions that will not result in white layer formation or will produce minimal white layer.

Recently, an interesting contribution has been made by Ramesh and Melkote [4] who presented a finite element model of continuous white layer formation. They modeled the problem as quenching by incorporating in the finite element (FE) model the effects of stresses and strains on the transformation temperature, volume expansion, and transformation plasticity. The study was conducted under thermally dominant cutting conditions that promote phase transformations.

By considering the relevance of the matter and the availability of limited presence of publications on the modeling of the white layer formation, in this paper, an empirical model to predict the microstructure changes has been proposed.

In particular, after brief remarks on the mechanisms related to the white layer formation, a finite element model to study the orthogonal cutting process on hardened AISI 52100 steel is proposed. The FE model was properly calibrated by means of an iterative procedure based on the experimental data concerning chip geometry, cutting forces, temperatures, and white layer.

Then, the proposed model was validated by comparing the predicted results with the experimental evidences found in the published literature.

Finally, a finite element analysis was carried out to analyze the influence of the principal process variables (cutting speed, uncut chip thickness, and material hardness) on the white layer formation.

2 Remarks on white layer formation

White layer formation is known to be a result of microstructural alteration on a martensite structure. It can be found in many material removal processes such as turning, reaming, grinding, and electrical discharge machining. The formation of a white layer and its quantification would indicate the amount of surface energy brought into the part/component. Currently, three different theories are prevalent to explain the structure of the white layer formation. According to Barry and Byrne [5] and Chou and Evans [3], the high austenite content of the surface white layer clearly confirms the occurrence of the reverse martensite transformation during machining. A rapid increase in temperature, combined with high pressure generated by the action of the tool, transforms the machined surface into an austenitic state. When the tool leaves, the surface cools down and the critical speed of martensite formation is reached by convection of heat into the air and by conduction into the workpiece material. As a result of the high speed, some austenite portions have no time to transform and some retained austenite traces can be found in the surface layer. Mybokwere et al. [6], Cho et al. [7], and Zhang et al. [8] showed that dynamic recovery is the dominant process in the formation of surface white layers and internal white adiabatic shear bands, and it can be explained simply as the beginning of dislocations. Assisted by the local increase in temperature due to rapid localized deformation, dislocations concentrate into tangles, producing regions of high and low dislocation density and forming sub-grain boundaries. Another hypothesis has been developed by Zurecki et al. [9] who assumed that there is an almost complete dissolution of carbides due to the high temperature generated by plastic deformation. As the tool leaves the material, the white layer cools down quickly, thus leading to the freezing of its microstructure. A small quantity of non-quenched martensite or retained austenite may develop within the white layer.

Among these three, the predominant effect on white layer formation seems to be coming from the first one. The predominant thermal effect on white layer formation was also confirmed by Habak et al. [10]. They demonstrated that the origin of the white layer in hard machining processes is in general thermo-mechanical and, more precisely, it is initially generated by a mechanical effect involving a localized shear force. Consequently, the high strain rate results in a localized temperature rise, generating a thermal effect that leads to the white layer formation.

Moreover, for the analysis of the mechanisms related to the white layer, it is essential to study the effects of process variables. For this reason, the principal observations taken from literature can be summarized as follows. Chou and Evans [3, 11] found that as a general trend, the white layer thickness increases with increasing cutting speed, and when the cutting speed reaches a critical value, the white layer depth slightly decreases or remains constant. They also showed that the depth of cut does not affect the white layer depth and that there is a slight increase with increasing uncut chip thickness.

The observations made by Chou and Evans [3, 11] were also confirmed by Chou and Song [12] who found that the variation of white layer depth is higher when the cutting speed is increased from 60 to 180 m/min, lower when the cutting speed varied from 180 to 240 m/min, and it tends to remain almost constant. Beyond this cutting speed, until 300 m/min, it shows a decrease in the white layer depth.

In addition, Chou and Song [12], for general cutting conditions, showed that the white layer depth increases with the increase in tool wear. Also, as far as the material hardness is concerned, Warren et al. [13] demonstrated that the white layer depth increases with the increase in material hardness. Finally, Guo and Schwach [14] verified that specimens without any microstructure modifications (i.e., no white layer formation) presented a longer life when compared to those with equivalent surface finish, but characterized by white layer formation.

3 Finite element model calibration

The present study is focused on calibration and validation of an empirical model for white layer prediction. The calibration strategy was carried out by means of a finite element analysis of machining process for a range of cutting speeds and workpiece hardness values and by comparing the predicted results with those found experimentally. In particular, the aim of this calibration phase was to determine the critical damage value (CDV), the shear factor (m), and the global heat transfer coefficient (h_{int}) at the tool–chip and tool–workpiece interfaces. Furthermore, the same iterative procedure was also utilized to empirically determine the coefficients J and $T_{\mathrm{phase\ transf}}$ to be set in the thermal-based white layer model (Fig. 1).

The FEM-based numerical procedure was developed to simulate the hard turning process based on the following assumptions:

1. Rigid cutting tool;
2. Isotropic hardening for workpiece material;
3. Non-isothermal elastic–viscoplastic material governed by incremental theory of plasticity and von Mises yield condition:

$$\overline{\sigma} = \frac{\sqrt{(\sigma_1 - \sigma_2)^2 + (\sigma_2 - \sigma_3)^2 + (\sigma_1 - \sigma_3)^2}}{\sqrt{2}} \quad (1)$$

where $\overline{\sigma}$ is the equivalent stress and σ_1, σ_2, and σ_3 are the principal stresses. The constitutive law, which describes the stress field with strain hardening effects, also takes into account the temperature, strain rate, and hardness effects. In particular, the latter effect needs to be present in the constitutive law since the proposed white layer model is empirically built on the hardness modification. Therefore, the hardness-based flow stress proposed by one of the present authors [13] was chosen and implemented in the current FE code:

$$\sigma\left(\varepsilon, \dot{\varepsilon}, T, HRc\right) = B(T)(C\varepsilon^n + F + G\varepsilon)\left[1 + \left(\ln\left(\dot{\varepsilon}\right)^m - A\right)\right] \quad (2)$$

where B is the temperature dependant factor, C represents the work hardening coefficient, F and G are two linear functions of hardness, and A is a material constant. The detailed procedure and the explanation for other terms in the above equation can be found in [15].

4. Brozzo's criterion [16] is employed to predict the effect of the stress on the chip segmentation during orthogonal cutting. Brozzo's criterion is expressed as:

$$\int_0^{\overline{\varepsilon}_f} \frac{2\sigma}{3(\sigma_1 - \sigma_m)} d\overline{\varepsilon} = D \quad (3)$$

where ε_f is the effective strain, σ_1 principal stress, σ_{m} the hydrostatic stress, and D the material constant representing resistance to failure (sometimes called "damage value"). Brozzo's criterion shows that when the integral of the left term (applied state) in Eq. 3 reaches the value of D (material state), the fracture occurs and the chip segmentation starts. This criterion is easy to use because only one material constant has to be determined. The other fracture damage criteria need two or more material constants to be determined.

5. Finally, as far as the white layer formation is concerned, a simple thermal model based on the hardness

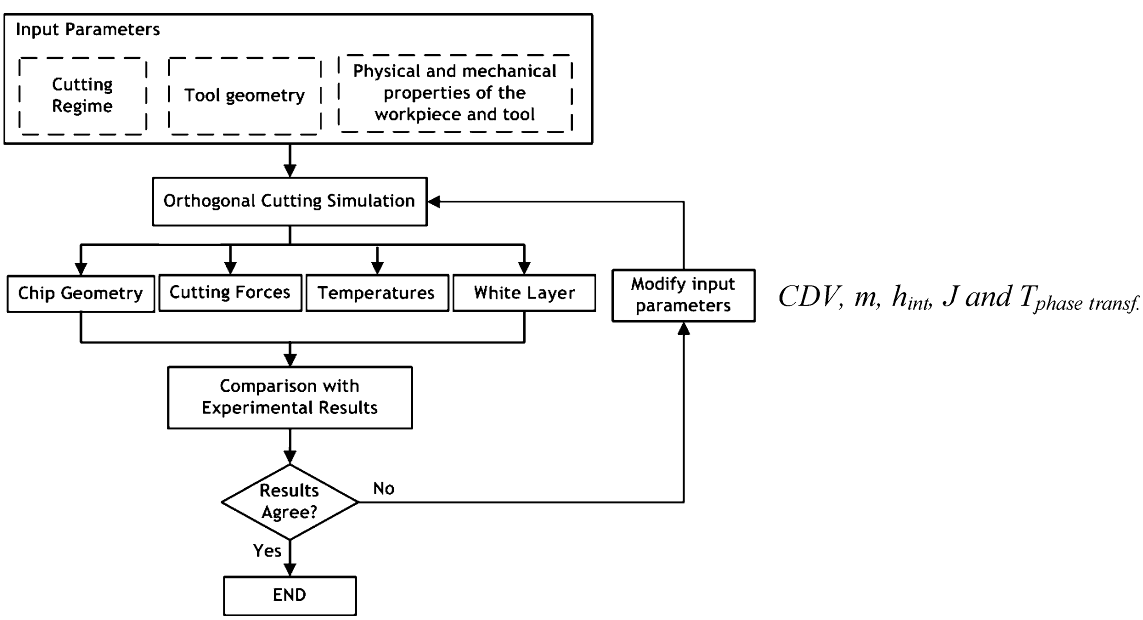

Fig. 1 The utilized iterative procedure for calibration phase

modification prevalent in the white layer was considered. This assumption was made by considering the results found by Ackan et al. [2] and Habak et al. [10] who demonstrated that white layer formation involves three steps: austenitization of the steel surface, followed by deformation of the high temperature austenite to large plastic strains, and finally, rapid quenching of the austenite by the bulk of the material to form a martensite structure. Therefore, the user routine implemented in the FE code is as follows:

$$\mathrm{HRC}_{\mathrm{Ref}} = \mathrm{HRC}_{\mathrm{Initial}}$$
$$\mathrm{IF}\ (T > T_{\mathrm{phase\ transf}})\ \mathrm{THEN}\ \Delta\mathrm{HRC} = J \times \left((67 - \mathrm{HRC}_{\mathrm{Initial}})/(1030 - T_{\mathrm{phase\ transf}}) \times (T - T_{\mathrm{phase\ transf}})\right)$$
$$\mathrm{ELSE}\ \Delta\mathrm{HRC} = 0.0$$
$$\mathrm{HRC}_{\mathrm{updated}} = \mathrm{HRC}_{\mathrm{Initial}} + \Delta\mathrm{HRC}$$
$$\mathrm{HRC}_{\mathrm{Ref}} = \mathrm{HRC}_{\mathrm{current\ step}}(\text{read from FEM at the current step})$$
$$\mathrm{IF}\ (\mathrm{HRC}_{\mathrm{updated}} > \mathrm{HRC}_{\mathrm{Ref}})\ \mathrm{THEN\ HRC} = \mathrm{HRC}_{\mathrm{updated}}\ (\text{new value to be used at the next step})$$
$$\mathrm{ELSE\ HRC} = \mathrm{HRC}_{\mathrm{Ref}}\ (\text{new value to be used at the nextstep})$$

where J and $T_{\mathrm{phase\ transf}}$, present in the ΔHRC function, were empirically found by the FE calibration, while the other constant values were derived from the continuous cooling transformation curve for the AISI 52100 [17]. Actually, quenching phenomenon is physically non-diffusive; thus, it is scientifically rigorous to simply apply the above reported user routine to predict the white layer formation.

It is also important to underline that the temperature is checked each step and for each element of the workpiece in order to update the current element hardness. The latter is stored before the next simulative Lagrangian step. Furthermore, it is also important to highlight that if the hardness variation happens, the material strength is locally harder than the bulk material, reflecting the reality of hard machining process.

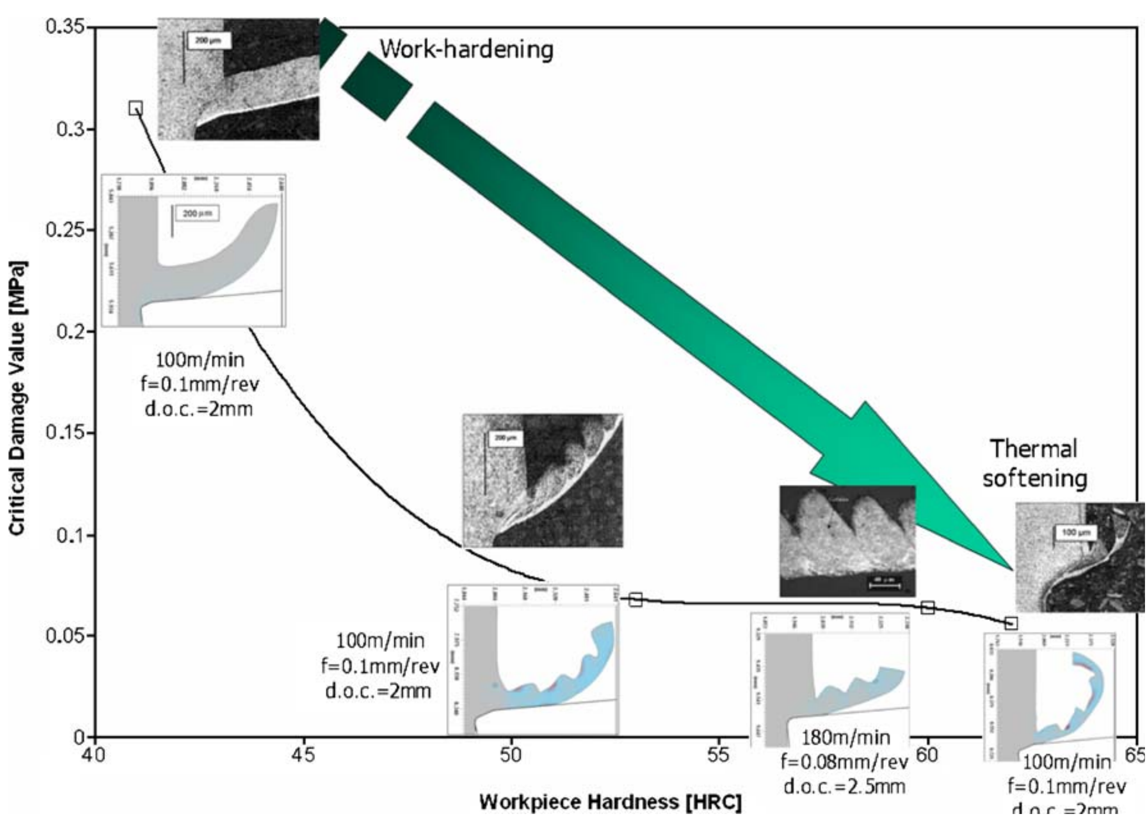

Fig. 2 The CDV diagrams obtained for AISI 52100 steel

Table 1 Experimentally measured [18] and numerically predicted cutting forces and maximum temperature on the chip

	Principal cutting force	Chip max temperature
Experimental results	1,702 N	613°C
Numerical results	1,568 N	640°C
Absolute err.%	7.9	4.4

The FE simulations were conducted for the same experimental conditions as those used by Habak et al. [18], Poulachon et al. [19, 20], and Ramesh et al. [21]. In particular, the experiments reported in [19, 20] were used for the calibration of the parameters CDV, J, and $T_{\text{phase transf.}}$ by an iterative procedure for determining the chip morphology and the white layer formation; the experimental evidence present in [18] was utilized to calibrate the shear factor m as well as the h_{int} at the tool–chip–workpiece interface.

3.1 Chip morphology calibration

Polachon et al. [19, 20] have experimentally shown that the two major parameters that influence chip morphology and segmentation are the hardness of the workpiece material and the cutting speed. Therefore, different cases were considered for the chip morphology calibration for combinations of these varying parameters. In particular, several workpiece hardness values (41HRC, 53HRC, 60HRC, 62HRC) and two cutting speeds (100 and 180 m/min) were considered. Also, two uncut chip thickness values (0.08 and 0.1 mm) were set and the tool geometries were chosen as those utilized in the experiments. The results of the chip morphology calibration process are discussed in detail in a previous research paper [13]. The calibration results confirm that as hardness increases, the fracture toughness (CDV) decreases (Fig. 2).

3.2 Calibration of cutting force and temperature

Prediction of both cutting forces and temperature become a key point in any machining processes, especially in hard machining, as demonstrated by Ghani et al. [22] and Ozel and Zeren [23]. Therefore, also in this research, prediction of the mentioned variables was carefully conducted. In particular, the comparison of the predicted and experimentally measured principal cutting force and maximum temperature measured on the chip is shown in Table 1 when the shear factor m and the h_{int} at the tool–chip–workpiece interfaces were imposed equal to 0.9 and 28 kW/m^2, respectively. The experimental results are from Habak et al. [18] for 150-m/min cutting speed, 0.1-mm/rev feed rate and 5-mm depth of cut. Hardness of the 52100 steel workpiece was 55 HRC. The cutting tool was a chamfered cBN insert (geometry: LCGN 160604-0600S-LF; grade: Seco CBN10) with a rake angle of −10°, a clearance angle of 7°, and a cutting edge radius of 15 μm.

3.3 Calibration of white layer formation

The last frame of the entire calibration procedure is referred to the white layer formation. The experimental observations are from the quick stop tests during cutting an AISI 52100

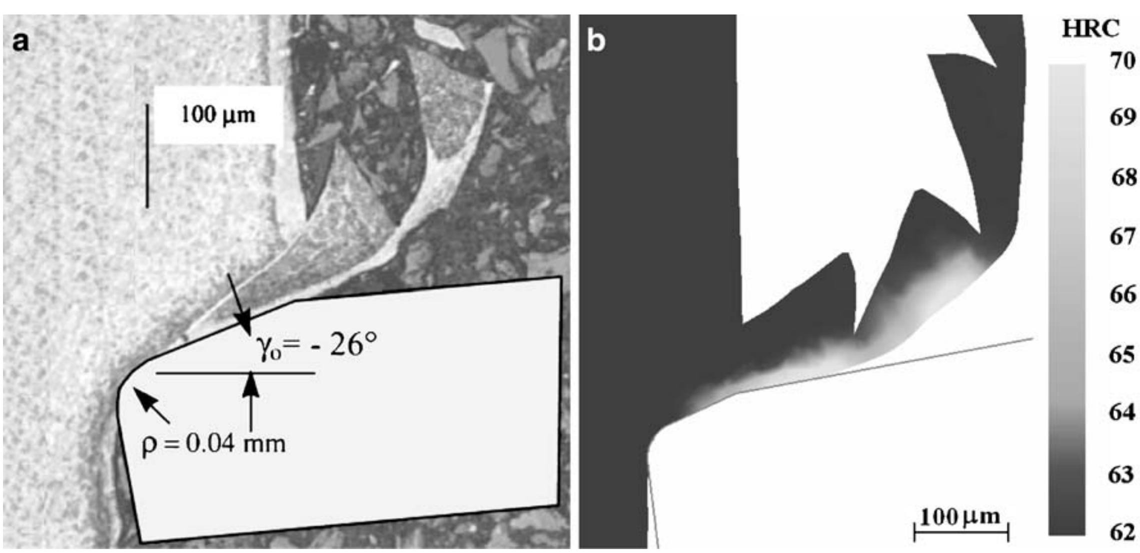

Fig. 3 Chip morphology and white layer formation during machining of AISI 52100 workpiece with an initial hardness of 62 HRC: **a** observed [20], **b** predicted

Table 2 Experimentally measured [20] and numerically predicted chip morphology, thickness of white layer formation, and hardness modification in the chip

	Chip morphology			White layer	
	$Pitch_{AVE}$ (μm)	$Peak_{AVE}$ (μm)	$Valley_{AVE}$ (μm)	$HRC_{max}/HRC_{initial}$	$Thickness_{AVE}$ (μm)
EXP results	112	157	23	1.15	25
NUM results	114	178	31	1.14	33
Absolute err.%	1.8	13.4	34.8	1	32

specimen (62HRC) conducted by Poulachon et al. [20]. The cutting parameters were: 100 m/min as cutting speed, 0.1 mm/rev as feed rate, and 1 mm as depth of cut. The utilized tool was a whisker-reinforced ceramic. Figure 3 and Table 2 report the calibration results including the relative errors estimated for chip shape, thickness of the white layer, and the hardness modification in this layer. These numerical results are referred to the final iterative step in which J and $T_{phase\ transf}$ parameters were found equal to 10° and 830°C, respectively.

It is important to highlight that $T_{phase\ transf}$ parameter is higher than that found by Ramesh [24] who found that the influence of stress and strain on the austenite start temperature due to high dislocation density associated with large strain produces an approximate austenite start temperature of 550–650°C. However, it is worth pointing out that the empirical model to describe the white layer formation, proposed in this research, was based on the assumption of a complete austenitization of the AISI 52100 workpiece.

4 Model validation

The FE model was validated by comparing numerical predictions from FE simulations with the experimental results found in [18, 21] for cutting forces, chip morphology, temperatures, and white layer formation for different cutting speeds, feeds, and material hardness values.

As far as the validation of principal cutting force, temperature, and chip morphology are concerned, the experimental observations obtained by Habak et al. [18] were utilized. The tool material and geometry are equal to those used in the calibration phase as well as the initial hardness and the feed when a different cutting speed (100 m/min) was used.

The comparison between the predicted and the experimental results are reported in Table 3 and Fig. 4.

The experimental results reported in [21] were utilized in order to verity the effectiveness of the proposed FE model for predicting the white layer formation on the machined surface. In particular, two cutting speeds, 183 m/min (case 1) and 274 m/min (case 2), were used when an AISI 52100 with 62HRC was machined using a cBN cutting tool (geometry: ANSI TNG-432; Kennametal KD050 grade: low-CBN content with ceramic binders). Both the feed rate and depth of cut were fixed at 0.127 mm/rev and 0.254 mm, respectively. Figure 5 shows the comparison between the predicted and the experimental results; the absolute errors are 12.8% for case 1 (20.3 μm for predicted average white layer thickness instead of 18 μm for the experimentally measured one) and 17.6% for case 2 (14.7 μm for predicted average white layer thickness instead of 12.5 μm for the experimentally measured one).

5 Finite element analysis of white layer formation

In this section, the influence of cutting parameters and initial hardness on white layer formation and, consequently, on the microstructure modifications will be discussed. In particular, three levels for each parameter were considered: 100, 200, and 300 m/min for the cutting speed; 0.1, 0.15,

Table 3 Experimentally measured [18] and numerically predicted chip morphology and principal cutting force

	Chip morphology			Principal cutting force (N)
	$Pitch_{AVE}$ (μm)	$Peak_{AVE}$ (μm)	$Valley_{AVE}$ (μm)	
EXP results	185	192	15.4	1,893
NUM results	170	216	19.3	1,762
Absolute err.%	8.1	12.5	25.3	6.9

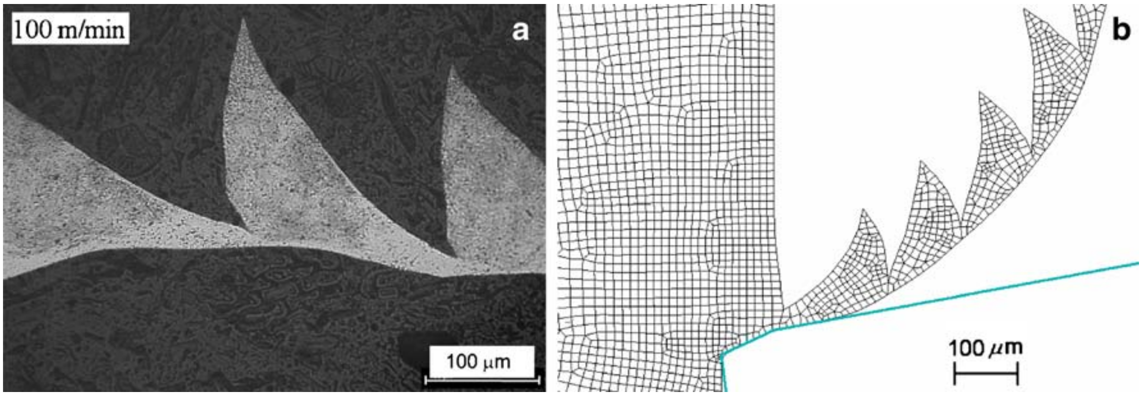

Fig. 4 Chip morphology during machining workpiece with an initial hardness of 55 HRC: **a** observed [18], **b** predicted

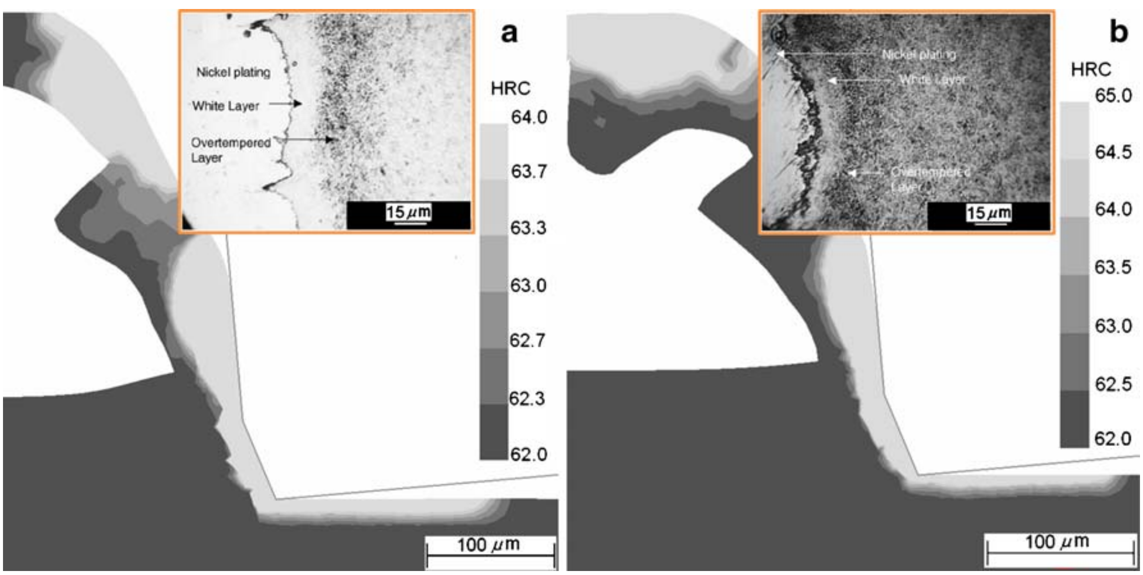

Fig. 5 Experimental [21] and predicted white layer on machined surface at two different cutting speeds: (**a**) 183 m/min, **b** 274 m/min

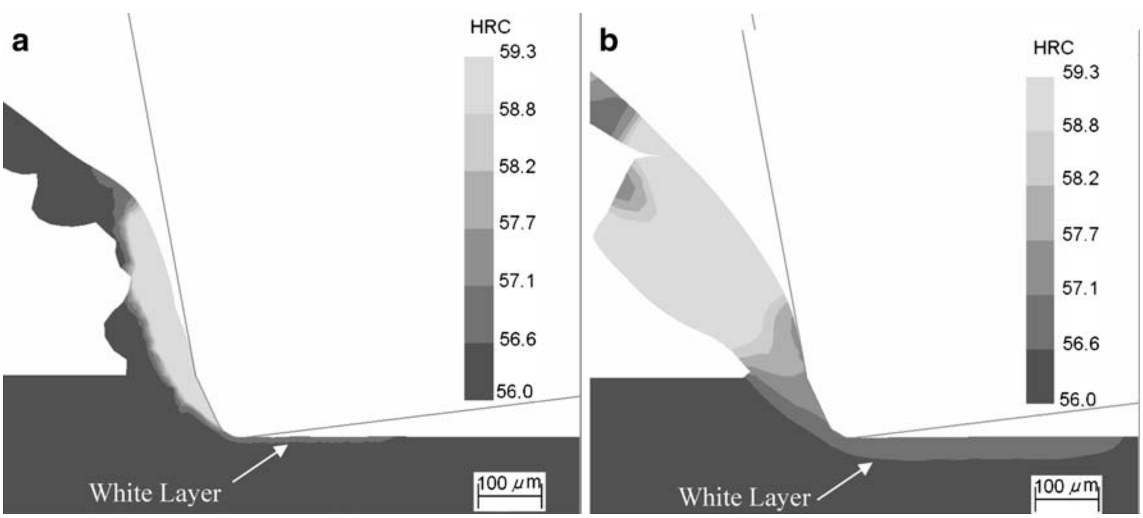

Fig. 6 Simulated white layer formation at different cutting speeds and fixed uncut chip thickness (0.1 mm) and initial hardness (56 HRC): **a** 200 m/min, **b** 300 m/min

Fig. 7 Influence of cutting speed on white layer depth: **a** t=0.10 mm, **b** t=0.15 mm, **c** t=0.20 mm

a

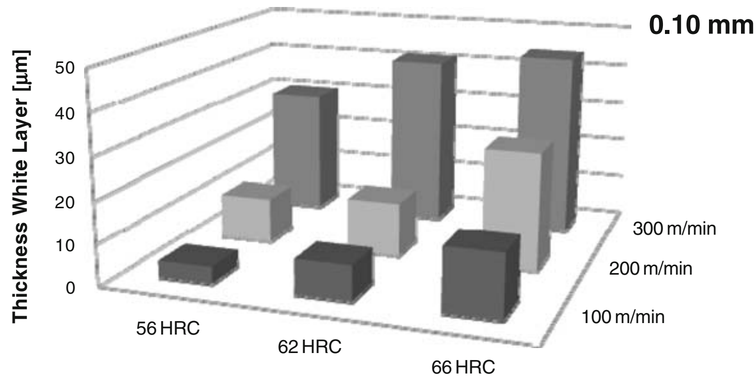

	56 HRC	62 HRC	66 HRC
100 m/min	4	8.3	15
200 m/min	10.8	13	28.1
300 m/min	30.3	41.2	44.2

b

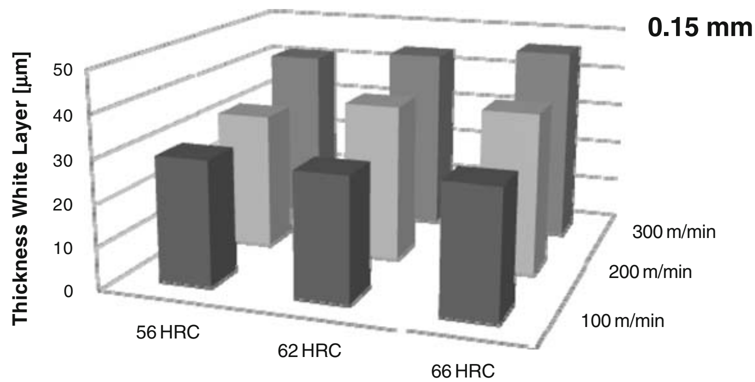

	56 HRC	62 HRC	66 HRC
100 m/min	29.2	28.8	29.6
200 m/min	32	36.8	37.6
300 m/min	41.2	43.6	46.1

c

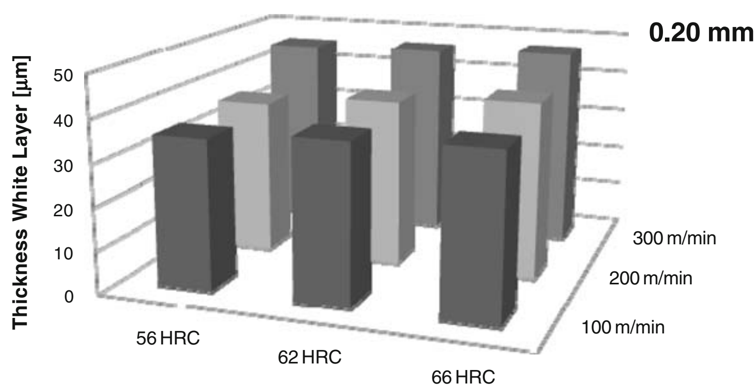

	56 HRC	62 HRC	66 HRC
100 m/min	35.1	37.3	38.3
200 m/min	36.4	39.1	41.2
300 m/min	45.4	46	47

and 0.2 mm for the uncut chip thickness; and finally, 56, 62, and 66 HRC for the initial workpiece hardness. The combination of the three levels provides a total of 27 numerical simulations which were conducted utilizing a fixed tool material: PCBN insert with 2 μm TiN thin layer (SNGA 12 04 08 S01020 7020).

5.1 Influence of cutting speed

In general, higher cutting speeds determine deeper microstructure modifications and, therefore, higher thickness of the white layer (Fig. 6), and this effect is more evident when lower uncut chip thickness and initial hardness were utilized (Fig. 7a).

In fact, from the observation of Fig. 7, the influence of cutting speed on the white layer depth tends to provide an almost constant value when higher initial hardness and, especially, at higher uncut chip thickness values (Fig. 7b, c).

These numerical observations are in agreement with those obtained experimentally by Han [25] concerning the increasing of white layer depth when initial workpiece hardness of 53–57 HRC and small uncut chip thickness (0.075–0.125 mm) are used. Also, the results are consistent with those experimentally found by Chou and Song [12] which showed that the variation of white layer depth is higher when the cutting speed changes from 60 to 180 m/min, lower when the cutting speed varied from 180 to 240 m/min, then it tends to remain almost constant until 300 m/min.

5.2 Influence of uncut chip thickness

The influence of the uncut chip thickness on white layer depth was studied, keeping a constant cutting speed and initial hardness. As seen in Fig. 8, the thickness of the white layer increases when increasing the uncut chip thickness, and this variation is more evident when a lower cutting speed is utilized. Furthermore, the white layer depth presents higher variations when the uncut chip thickness increases from 0.1 to 0.15 mm (Fig. 9).

This effect is more evident at 100 and 200 m/min, while at 300 m/min, it tends to show similar thickness especially when the initial workpiece hardness values of 62 and 66 HRC are considered (Fig. 9b, c). Moreover, the numerical results underline that the above trends seem to be independent of the initial workpiece hardness. The predicted results are qualitatively in agreement compared with the experimental observations reported in [13] as far as the trends are concerned. On the contrary, they diverge from experimental data since the prediction furnishes higher white layer penetration. The reason of this divergence is the absence of the tempering effect in the user routine. In other words, since the over-tempered martensite is not taken into account in this work, the prediction of the white layer thickness is numerically overestimated, especially when severe cutting conditions for hard turning and higher hardness material states are utilized.

5.3 Influence of initial hardness

The influence of the initial workpiece hardness on white layer depth and microstructure modifications was investigated, keeping both the cutting speed and the uncut chip thickness constant. As shown in Fig. 10, the white layer depth increases when increasing the initial hardness, and this variation is more evident when an uncut chip thickness of 0.1 mm is used. In fact, when both the uncut chip thickness and the cutting speed are higher than 0.15 mm and 200 m/min, respectively, a different initial hardness does not generate any significant increment of the white layer depth regardless of the values of cutting speed and uncut chip thickness imposed as illustrated in Fig. 11.

These numerical predictions are once more very similar to those found in the earlier experimental investigations [13].

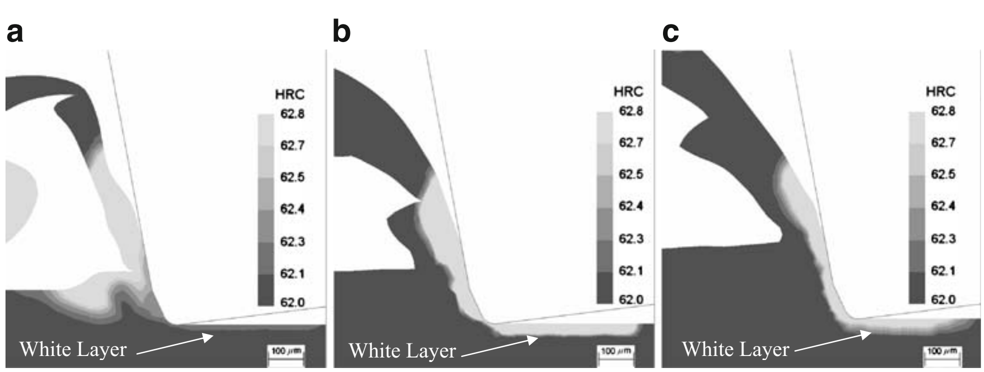

Fig. 8 Simulated white layer formation at different uncut chip thickness and fixed cutting speed (200 m/min) and initial hardness (62 HRC): **a** t=0.10 mm, **b** t=0.15 mm, **c** t=0.20 mm

Fig. 9 Influence of uncut chip thickness on white layer depth: **a** 56 HRC, **b** 62 HRC, **c** 66 HRC

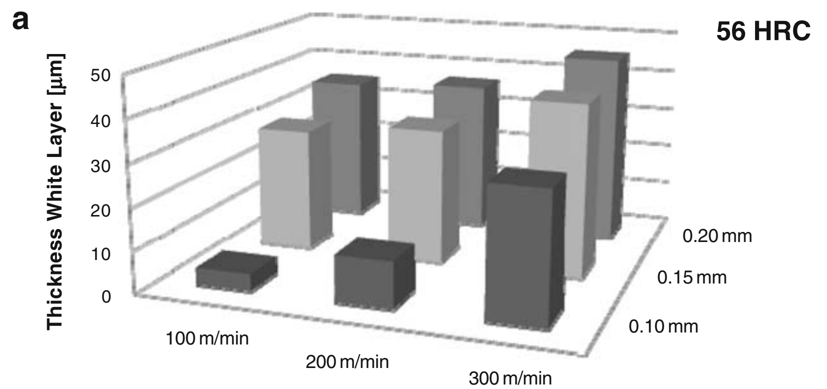

	100 m/min	200 m/min	300 m/min
■ 0.10 mm	4	10.8	30.3
■ 0.15 mm	29.2	32	41.2
■ 0.20 mm	35.1	36.4	45.4

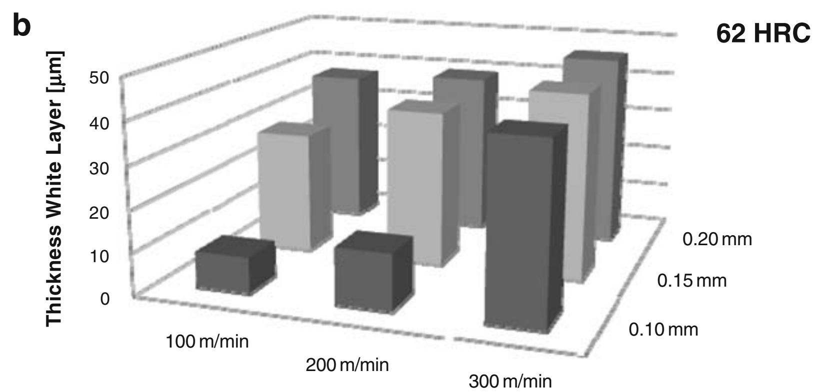

	100 m/min	200 m/min	300 m/min
■ 0.10 mm	8.3	13	41.2
■ 0.15 mm	28.8	36.8	43.6
■ 0.20 mm	37.3	39.1	46

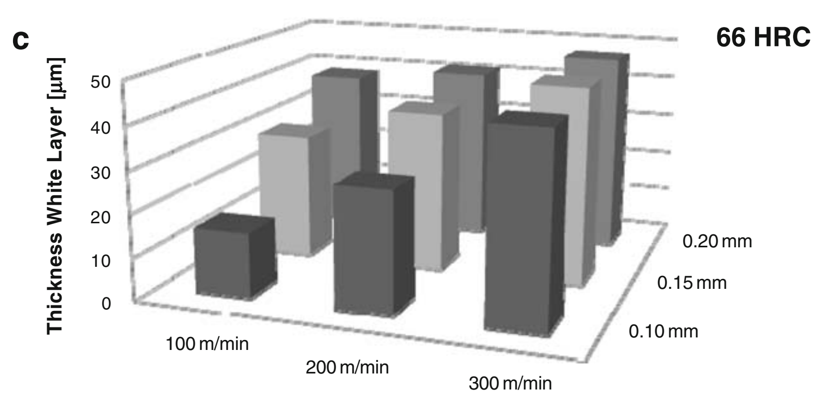

	100 m/min	200 m/min	300 m/min
■ 0.10 mm	15	28.1	44.2
■ 0.15 mm	29.6	37.6	46.1
■ 0.20 mm	38.3	41.2	47

Fig. 10 Influence of initial material hardness on white layer thickness: **a** 100 m/min, **b** 200 m/min, **c** 300 m/min

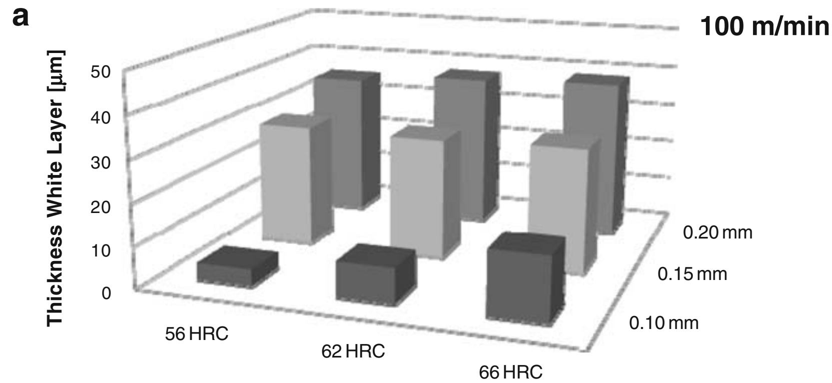

	56 HRC	62 HRC	66 HRC
0.10 mm	4	8.3	15
0.15 mm	29.2	28.8	29.6
0.20 mm	35.1	37.3	38.3

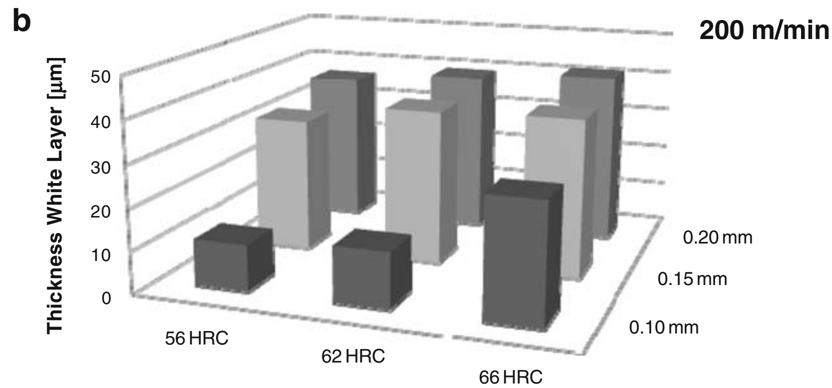

	56 HRC	62 HRC	66 HRC
0.10 mm	10.8	13	28.1
0.15 mm	32	36.8	37.6
0.20 mm	36.4	39.1	41.2

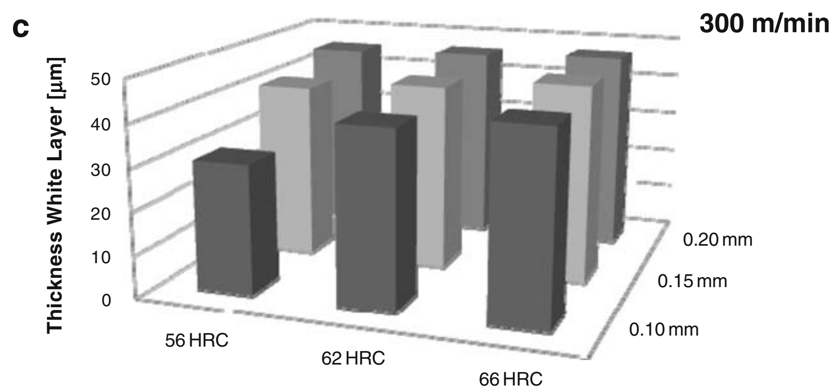

	56 HRC	62 HRC	66 HRC
0.10 mm	30.3	41.2	44.2
0.15 mm	41.2	43.6	46.1
0.20 mm	45.4	46	47

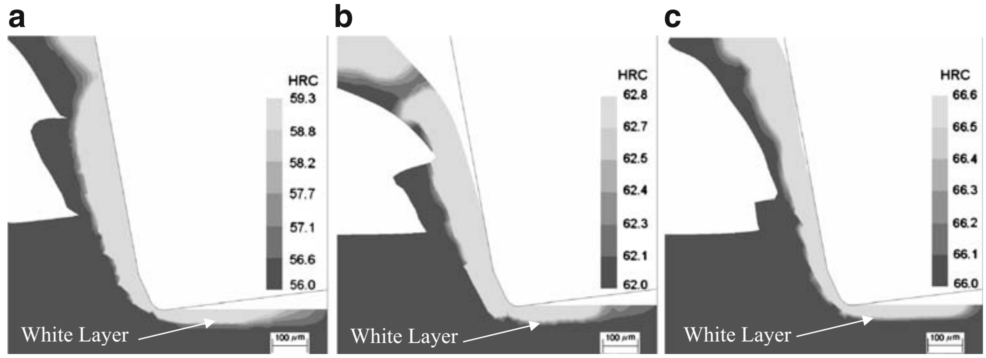

Fig. 11 Simulated white layer formation at different initial hardness and fixed cutting speed (300 m/min) and uncut chip thickness (0.20 mm): **a** 56 HRC, **b** 62 HRC, **c** 66HRC

Another important issue that can be investigated using this FE analysis is the modification of metallurgical material state on the machined surface due to the white layer formation. It is well known that the hardness on the white layer is higher than the bulk material hardness. Therefore, an important parameter to investigate is the ratio $HRC_{max}/HRC_{initial}$ where the HRC_{max} represents the maximum hardness value measured on the white layer after its formation, while $HRC_{initial}$ corresponds to the initial workpiece hardness which is constant in the bulk material

As seen in Fig. 12, when increasing the initial workpiece hardness, the parameter $HRC_{max}/HRC_{initial}$ decreases. This tendency is more evident when higher uncut chip thickness and cutting speeds are utilized and kept constant. Moreover, higher $HRC_{max}/HRC_{initial}$ values are observed when the initial hardness ranges between 56 and 62 HRC. Furthermore, these numerical results are very similar in trends to those experimentally observed by Poulachon et al. [20].

6 Conclusions

This paper presents a FE model which was used in the study of hard turning of AISI 52100 steel in term of chip morphology, cutting forces, temperature, and white layer formation. For the white layer formation, a simple model was empirically built and was proposed. This model, as well as the entire FE model, was calibrated and validated for a series of experimental observations. The reasonable agreement obtained between the experimental and numerical results indicate that the proposed FEM model is suitable for studying the influence of cutting parameters and initial hardness on white layer formation during hard machining of AISI 52100 steel. It was observed that the white layer depth increases with both the cutting parameters and the initial hardness, and some combinations of cutting parameters and initial hardness values can however generate different trends. Indeed, cutting speeds up to 250–300 m/min show a slightly increment when compared to lower cutting speeds, while for speeds higher than 300 m/min, the white layer remains constant or slightly decreases in some cases.

However, within the range of investigated cutting parameters and initial hardness values, the combination of the highest above process variables seems to have the largest influence on white layer depth.

The modifications of metallurgical material state (different hardness values generated on the white layer) also follow the experimental observations [20], showing that the ratio $HRC_{max}/HRC_{initial}$ decreases when the resistance of the bulk material increases.

Finally, it should be pointed out that other complex metallurgical features such as dark layer formation in the workpiece were not considered at this stage, and a further investigation on this topic will be necessary to improve the accuracy of the model.

Also, important metallurgical aspects such as the transformation of microstructure, including the topological parameters such as the grain size, grain elongation, etc., are being considered in our current investigations which will be reported later.

Acknowledgments The authors gratefully acknowledge Dr. Mike Foster and Dr. Chris Fischer by STFC-Deform, Columbus (OH) for their support in developing the FE model. The authors would also to thank Dr. Stefania Rizzuti for her technical contribution in developing this study.

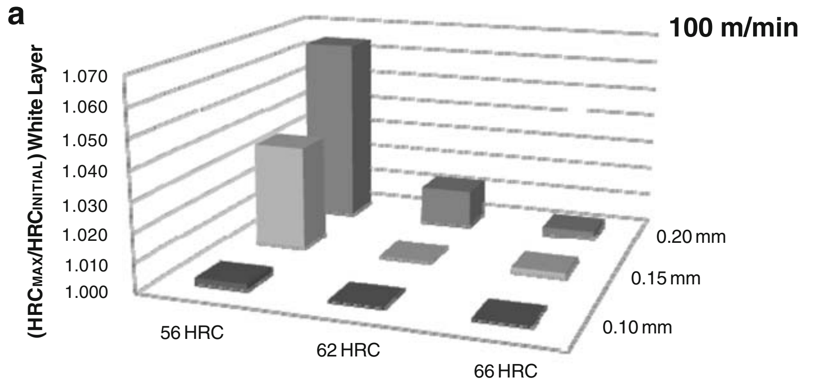

	56 HRC	62 HRC	66 HRC
■ 0.10 mm	1.002	1.000	1.000
■ 0.15 mm	1.036	1.000	1.002
■ 0.20 mm	1.064	1.013	1.002

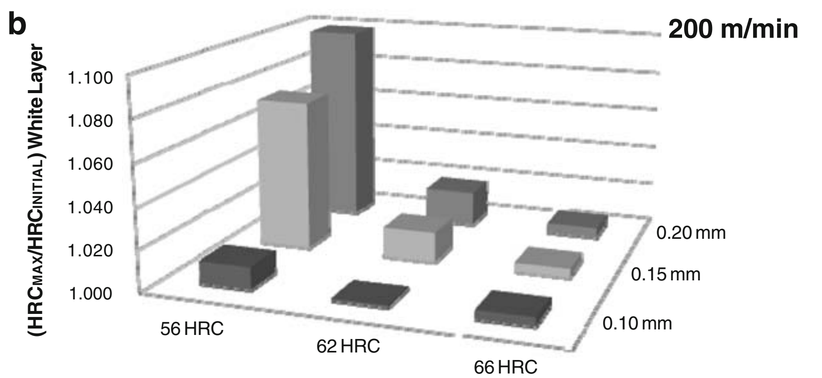

	56 HRC	62 HRC	66 HRC
■ 0.10 mm	1.011	1.001	1.004
■ 0.15 mm	1.073	1.015	1.004
■ 0.20 mm	1.098	1.018	1.005

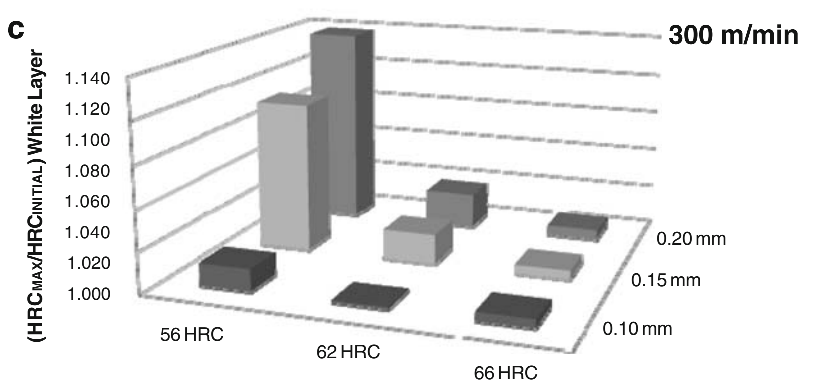

	56 HRC	62 HRC	66 HRC
■ 0.10 mm	1.018	1.019	1.009
■ 0.15 mm	1.107	1.024	1.014
■ 0.20 mm	1.125	1.029	1.015

Fig. 12 Hardness modification on white layer due to different initial heat treatment condition: **a** 100 m/min, **b** 200 m/min, **c** 300 m/min

References

1. Akcan NS (1998) Microstructure analysis and temperature modelling in finish machining of hardened steels. MS thesis, School of Industrial Engineering, Purdue University
2. Akcan NS, Shah S, Moylan SP, Chhabra PN, Chandrasekar S, Farris TN (1999) Characteristics of white layers formed in steels by machining. Manuf Sci Eng 10:789–795
3. Chou YK, Evans CJ (1999) White layers and thermal modeling of hard turned surfaces. Int J Mach Tools Manuf 39:1863–1881 doi:10.1016/S0890-6955(99)00036-X
4. Ramesh A, Melkote SN (2008) Modeling of white layer formation under thermally dominant conditions in orthogonal machining of hardened AISI 52100 steel. Int J Mach Tools Manuf 48:402–414 doi:10.1016/j.ijmachtools.2007.09.007
5. Barry J, Byrne G (2002) TEM study on the surface white layer in two turned hardened steels. J Mater Sci Eng A 325:356–364 doi:10.1016/S0921-5093(01)01447-2
6. Mybokwere CO, Nutt SR, Duffy J (1994) Shear band formation in 4340 steel: a TEM study. Mech Mater 17:97–110 doi:10.1016/0167-6636(94)90052-3
7. Cho KM, Lee S, Nutt SR, Duffy J (1993) Adiabatic shear band formation during dynamic torsional deformation of an HY-100 steel. Acta Metall Mater 41(3):923–932 doi:10.1016/0956-7151(93)90026-O
8. Zhang B, Shen W, Liu Y, Tang X, Wang Y (1997) Microstructures of surface white layer and internal white adiabatic shear band. Wear 211:164–168 doi:10.1016/S0043-1648(97)00099-9
9. Zurecki Z, Ghosh R, Frey JH (2003) Investigation of white layers formed in conventional and cryogenic hard turning steels. Proceedings of IMECE'03, 2003 ASME International Mechanical Engineering Congress and Exposition, Washington, DC, November 16–21
10. Habak M, Lebrun JL, Morel A (2007) A study of the influence of the metallurgical state on shear band and white layer generation in 100Cr6 steel: application to machining. Proceedings of the 10th ESAFORM Conference on Material Forming, Zaragoza, Spain, 18–20 April, pp 691–696
11. Chou YK, Evans CJ (1998) Process effects on white layer formation in hard turning. Trans NAMRI SME 26:117–122
12. Chou YK, Song H (2005) Thermal modeling for white layer prediction in finish hard turning. Int J Mach Tools Manuf 45:481–495 doi:10.1016/j.ijmachtools.2004.09.006
13. Warren AW, Guo YB, Weaver ML (2006) The influence of machining induced residual stress and phase transformation on the measurement of subsurface mechanical behaviour using nano-indentation. Surf Coat Tech 200:3459–3467 doi:10.1016/j.surfcoat.2004.12.028
14. Guo YB, Schwach DW (2005) An experimental investigation of white layer on rolling contact fatigue using acoustic emission technique. Surf Coat Technol 27:1051–1061
15. Umbrello D, Hua J, Shivpuri R (2004) Hardness based flow stress for numerical modeling of hard machining AISI 52100 bearing steel. Mater Sci Eng A 347:90–100 doi:10.1016/j.msea.2004.01.012
16. Brozzo P, De Luca B, Rendina R (1972) A new method for the prediction of formability limit of metal sheet. Proceedings of the 7th Biennial Conference of the International Deep Drawing Research Group
17. ASM International (1991) Heat treating of steels and surface hardening of steel. ASM Handbook vol. 4, Heat Treating
18. Habak M, Lebrun JL, Huneau B, Germain G, Robert P (2006) Effect of carbides and cutting parameters on chip morphology and cutting temperature during orthogonal hard turning of 100Cr6 bearing steel with a cBN cutting tool. Proceedings of the 9th CIRP International Workshop on Modeling of Machining Operations. Bled, Slovenia, 11–12 May, pp 517–524
19. Poulachon G, Moisan A (2000) Hard turning: chip formation mechanisms and metallurgical aspects. ASME J Manuf Sci Eng 122:407–412 doi:10.1115/1.1285891
20. Poulachon G, Moisan A, Jawahir IS (2001) Tool wear mechanisms in hard turning with polycrystalline cubic boron nitride tools. Wear 250:576–586 doi:10.1016/S0043-1648(01)00609-3
21. Ramesh A, Melkote SN, Allard LF, Riester L, Watkins TR (2005) Analysis of white layers formed in hard turning of AISI 52110 steel. Mater Sci Eng A 390:88–97 doi:10.1016/j.msea.2004.08.052
22. Ghani MU, Abukhshim NA, Sheikh MA (2008) An investigation of heat partition and tool wear in hard turning of H13 tool steel with CBN cutting tools. Int J Adv Manuf Technol 39(9–10):874–888 doi:10.1007/s00170-007-1282-7
23. Ozel T, Zeren E (2007) Finite element modeling the influence of edge roundness on the stress and temperature fields induced by high-speed machining. Int J Adv Manuf Technol 35(3–4):255–267 doi:10.1007/s00170-006-0720-2
24. Ramesh A (2002) Prediction of process-induced microstructural changes in orthogonal hard machining. PhD thesis, Mechanical Engineering, Georgia Institute of Technology
25. Han S (2006) Mechanisms and modelling of white layer formation in orthogonal machining of steels. PhD thesis, Mechanical Engineering, Georgia Institute of Technology